Structural Dynamic Model Obtained From Flight for Use With Piloted Simulation and Handling Qualities Analysis

Bruce G. Powers

June 1996

Structural Dynamic Model Obtained From Flight for Use With Piloted Simulation and Handling Qualities Analysis

Bruce G. Powers
Analytical Services & Materials, Inc.
Edwards, California

.

ABSTRACT

The ability to use flight data to determine an aircraft model with structural dynamic effects suitable for piloted simulation and handling qualities analysis has been developed. This technique was demonstrated using SR-71 flight test data. For the SR-71 aircraft, the most significant structural response is the longitudinal first-bending mode. This mode was modeled as a second-order system, and the other higher order modes were modeled as a time delay. The distribution of the modal response at various fuselage locations was developed using a uniform beam solution, which can be calibrated using flight data. This approach was compared to the mode shape obtained from the ground vibration test, and the general form of the uniform beam solution was found to be a good representation of the mode shape in the areas of interest. To calibrate the solution, pitch-rate and normal-acceleration instrumentation is required for at least two locations. With the resulting structural model incorporated into the simulation, a good representation of the flight characteristics was provided for handling qualities analysis and piloted simulation.

INTRODUCTION

Performance requirements generally call for a structure to be as light as possible. For large cruise vehicles, such as the high-speed civil transport and single-stage-to-orbit vehicles, maneuvering requirements are generally low. The combination of low maneuvering requirements with a high vehicle gross weight often results in a relatively flexible structure where the frequencies of the structural modes approach those of the rigid-body modes. Therefore, it is highly desirable to include the structural modes in the analysis of the handling qualities and the piloted simulation of the vehicle. A simulator study of a vehicle that included structural dynamic modes[1] concluded that structural dynamics can have a significant effect on the handling qualities of the vehicle. However, most piloted simulations do not include structural dynamic modes primarily because of the complexity of the structural modes. For a full-envelope simulation, the structural mode calculations can be of a similar order of magnitude as those for the rigid-body modes, which can often tax the capability of the simulation computers.

Another difficulty arises when providing simulation support for flight research programs. In this case, the structural modes that are available from either a prediction or ground vibration test (GVT) often do not correspond to the current configuration being tested. It is generally not feasible from a cost and time standpoint to update the structural dynamic models to support handling qualities experiments. The goal of this study was to develop an easy method to implement a structural model that can be calibrated with flight data. Because this model is being developed to support piloted simulation and handling qualities analysis, it was preferred to have comparatively fewer instrumentation and flight test maneuvers than for the handling qualities experiment itself. This report documents the development and calibration of the structural models using actual flight test data.

In the SR-71 program, the flight data have shown a noticeable structural response. The structural modes have generally not been modeled in the simulations or past handling qualities analyses. Many handling qualities criteria today depend on frequency response characteristics that generally extend to frequencies that include some structural dynamic mode effects. As a result, it was necessary to expand the current SR-71 models to include structural dynamic effects. The first fuselage bending dynamics were easy to distinguish. Although the pilots were very conscious of the structural dynamic motion, it was not a handling qualities problem because the motion was far enough removed from the rigid-body frequencies. The mode was well enough defined and of sufficient magnitude that it could be used to develop the modeling method for incorporating the structural dynamic effects. The SR-71 aircraft was used to validate the simulation and analysis capability. This modeling technique provides the capability to use flight data to establish structural models suitable for simulation and analytical studies that will be applicable to other large, flexible vehicles of the future.

NOMENCLATURE

A_n	normal acceleration, g
A_1	mode shape bias
A_2	mode shape angular scaling factor
$c.g.$	center of gravity, percent
C_{F_δ}	control surface input effectiveness coefficient, per deg
dz/dx	slope of normalized structural mode vertical deflection
F_δ	control surface input effectiveness, in/deg
FS	fuselage station, in.
FS_0	reference fuselage station, in.
g	acceleration caused by gravity, ft/sec^2
GVT	ground vibration test
K_1	displacement constant
K_2	slope constant
L	characteristic length, ft
L_α	rigid-body lift caused by angle of attack, 1/sec
L_δ	rigid-body lift caused by elevator, 1/sec
M	Mach number
M_q	rigid-body pitching acceleration caused by pitch rate, 1/sec
M_α	rigid-body pitching acceleration caused by angle of attack, 1/sec
M_δ	rigid-body pitching acceleration caused by elevator, 1/sec
q	pitch angular rate, deg/sec
$\bar{q}$	dynamic pressure, lb/ft^2
$\dot{q}$	pitch angular acceleration, deg/sec^2
s	Laplace operator
S	wing area, ft^2
SAS	stability augmentation system
V	velocity, ft/sec
W	aircraft gross weight, lb
x	horizontal axis coordinate, ft
z	vertical displacement, in.
$\dot{z}$	vertical velocity, in/sec
δ	elevator deflection, deg
$\dot{\delta}_p$	pilot stick input, in.
Δx	distance from center of gravity to sensor, ft
$\Delta\delta$	incremental elevator deflection from trim, deg

ζ	damping ratio
η	structural modal displacement, in.
$\dot{\eta}$	structural modal velocity, in/sec
$\ddot{\eta}$	structural modal acceleration, in/sec^2
θ	pitch angle, deg
τ_{a_n}	normal-acceleration time delay, sec
τ_δ	elevator time delay, sec
ω	natural frequency, rad/sec

Subscripts

aft	aft instrumentation location
d	delayed
fwd	forward instrumentation location
r	rigid value
s	structural value
0	bias term

STRUCTURAL DYNAMIC MODEL

The most significant structural dynamic response of the SR-71 aircraft is the longitudinal first-bending mode. Figure 1 shows the flight-measured pitch rate and normal acceleration caused by a sharp, longitudinal pitch stick input as well as the rigid-body motion obtained from the simulation response to the same input. The flight response
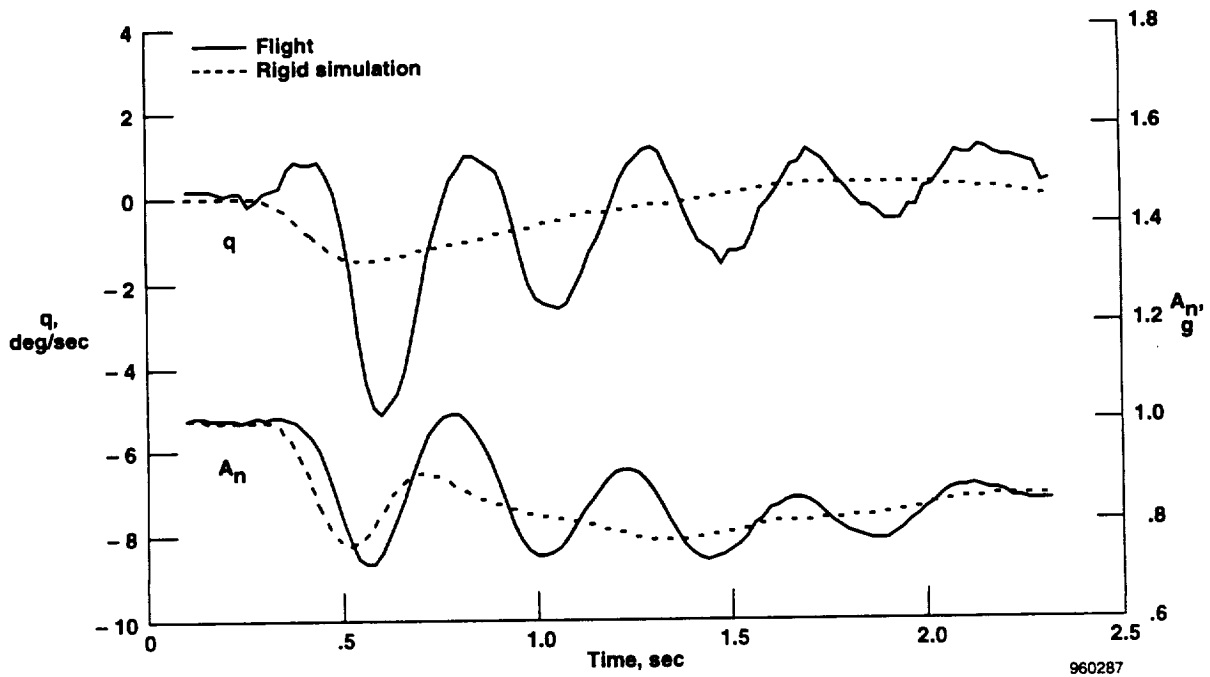

Figure 1. Comparison of flight response at forward-sensor location with rigid-body simulation response.

3

has a considerable additional higher frequency component because of the structural response. A structural response of this type can be described by the product of the dynamic response of the mode and the spatial distribution of the structural mode (i.e., the mode shape):

$$z = \eta \ K_1(x)$$

The dynamic portion of the response, η, is the response at one point along the fuselage, usually of maximum amplitude. The mode shape, $K_1(x)$, is the distribution of the response for other locations along the fuselage. The exact distribution of the deflection can be obtained from a structural analysis using the actual mass and structural characteristics from a GVT or from flight data. In general, the distribution would be a function of loading and flight condition. In the following section, an approximate distribution will be developed based on the solution for a uniform beam. It will be shown that this distribution provides a reasonable representation of the structural mode for the purpose of performing handling qualities analysis. Flight data can be used to calibrate the approximate solution with a minimum of instrumentation to provide the best match of the actual vehicle as tested.

Mode Shape Model

The displacement constant, K_1, is the distribution of the response for locations along the fuselage. For a uniformly loaded beam, the displacement constant is a sinusoidal function:

$$K_1 = \sin(p \ x/L + \phi) + A_1$$

The nodes of the first-bending mode are located at $x = 0.224L$ and at $x = 0.776L$, where L is the beam length.[2] The other constants are $p = 1.5\pi$, $\phi = 0.75\pi$, and $A_1 = 0.267$. The primary variable is the nondimensional beam length x/L. Figure 2 illustrates the resulting mode shape.
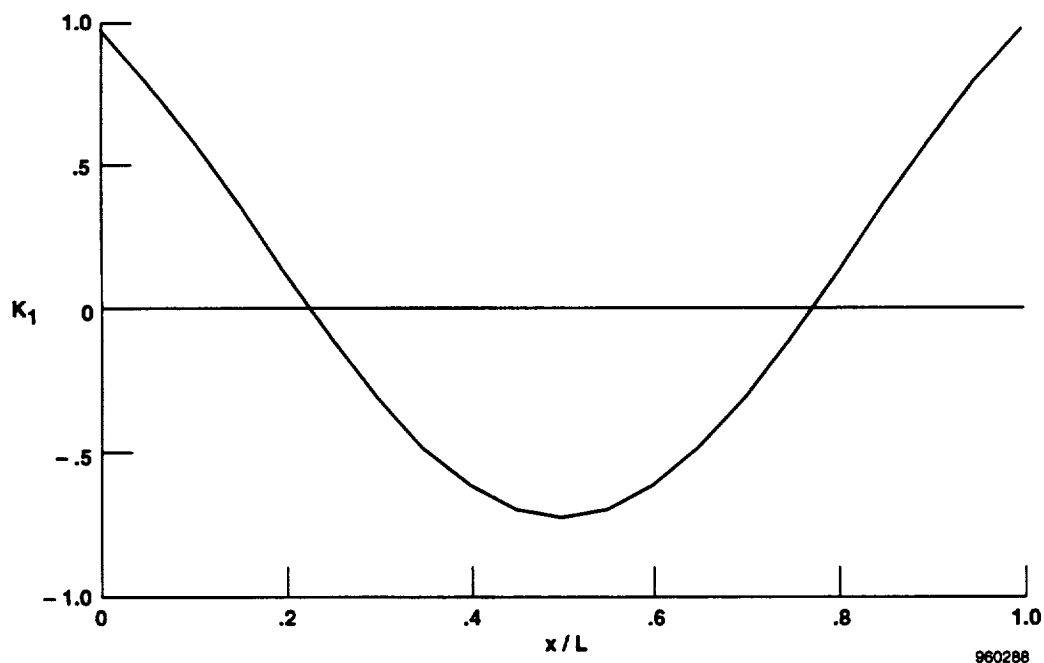

Figure 2. Mode shape for uniformly loaded beam.

The uniform beam solution has three variables that can be used to fit a particular mode shape: L, p, and A_1. The form of the solution can be rearranged slightly to provide more meaningful parameters. Because the structural coordinate system of the uniform beam solution is not necessarily coincident with the aircraft coordinate system, a bias between the two coordinate systems is required so that $x = (FS - FS_0)/12$, where FS is the fuselage station of the aircraft reference system in inches. For easier interpretation of the variables, it is useful to change the phase parameter so that FS_0 corresponds to the center of the beam where the slope is zero. The resulting expression for the deflection constant is as follows:

$$K_1 = -\cos\left(1.5\pi\frac{FS - FS_0}{12L}\right) + A_1$$

To test the validity of the assumption that a uniformly loaded beam solution can reasonably represent an actual aircraft mode shape, this form of solution was used to fit the mode shape obtained from a GVT. The GVT data obtained from the YF-12 aircraft,[3] which is geometrically similar to the current SR-71 test aircraft, provide a definition of the shape of the first-bending mode. A curve fit of the data was obtained using the sinusoidal form of the uniform beam solution. Figure 3 shows the GVT data and the curve fit. The fit of the GVT data results in an effective length of 139 ft (compared to the actual fuselage length of 107 ft) and an inflection point location of FS_0 798. The bias, A_1, was 0.72 rather than the uniform beam solution of 0.267. The uniform beam form of solution provides a good fit of the actual aircraft deflection curve from the GVT data, except near the aft end of the airplane. For handling qualities analysis, the range of interest is from the nose to the center of gravity (c.g.) location (FS 900), which encompasses the pilot location, control system, and instrumentation sensors.
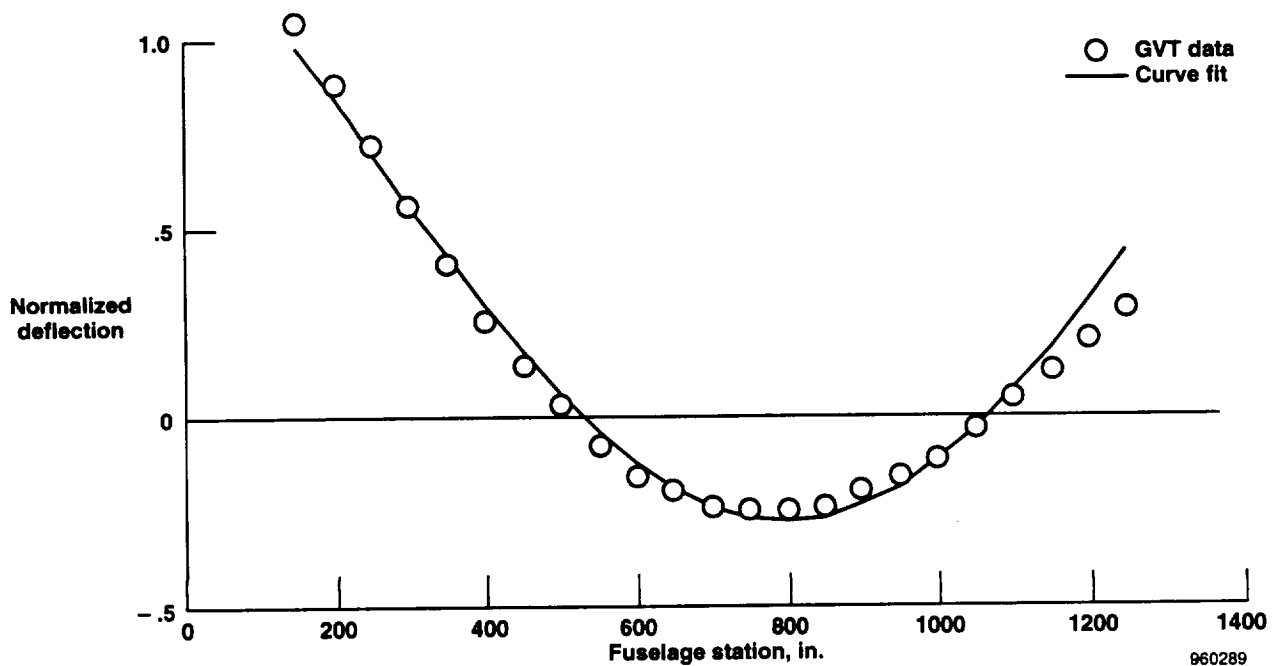

Figure 3. Fit of GVT data using form of uniform beam solution.

5

Dynamic Response Model

The dynamic portion of the response, η, is modeled as a second-order system with the elevator as the forcing function:

$$\ddot{\eta} + 2\,\zeta\,\omega\,\dot{\eta} + \omega^2\,\eta \;=\; \omega^2\,F_\delta\,\Delta\delta$$

The term F_δ is the effectiveness of the elevator which, in conjunction with the normalized deflection K_1, scales the structural deflection response z_s in inches when the elevator input is in degrees. The pitch angular deflection of the structure is the slope of the deflection curve with respect to the longitudinal distance and is given by the following:

$$dz/dx \;=\; -K_2\,\eta$$

The slope dz/dx is approximately the angle of the fuselage relative to the rigid-body x-axis.* The slope constant, K_2, is given by the following:

$$K_2 \;=\; \frac{-A_2}{L}\sin\!\left(1.5\pi\frac{FS-FS_0}{12L}\right)$$

The scale factor, A_2, provides the proper scaling for the pitch angle equations. The structural dynamic displacements and angles are perturbations from the rigid-body values. The structural dynamic components of the various response parameters are as follows:

Displacements: $\quad z_s = K_1\,\eta \quad$ (in.) $\qquad \theta_s = K_2\,\eta \quad$ (deg)

Rates: $\quad \dot{z}_s = K_1\,\dot{\eta} \quad$ (in/sec) $\quad q_s = K_2\,\dot{\eta} \quad$ (deg/sec)

Accelerations: $\quad A_{n_s} = \dfrac{K_1}{12g}\ddot{\eta} \quad$ (g) $\qquad \dot{q}_s = K_2\,\ddot{\eta} \quad$ (deg/sec^2)

For the nonlinear simulation, the elevator input to the structural mode, $\Delta\delta$, is the incremental elevator deflection from trim. The effects of static structural deflections are included in the basic aerodynamic model, which contains the static aeroelastic corrections. The complete equations for the two types of measured parameters that were available on the test aircraft, normal acceleration and pitch rate, are as follows:

$$A_{n_s} \;=\; \frac{1}{12g}\left[-\cos\!\left(1.5\pi\frac{(FS-FS_0)}{12L}\right)+A_1\right]\left[\frac{s^2\,\omega^2}{s^2+2\omega\zeta s+\omega^2}\right]F_\delta\,\Delta\delta$$

$$q_s \;=\; \left[\frac{-A_q}{L}\sin\!\left(1.5\pi\frac{(FS-FS_0)}{12L}\right)\right]\left[\frac{s\,\omega^2}{s^2+2\omega\zeta s+\omega^2}\right]F_\delta\,\Delta\delta$$

The structural dynamics are then added to the rigid-body motion to obtain the total vehicle response. To account for the effects of higher order structural modes that have not been modeled, a time delay was introduced between the elevator deflection and the input to both the rigid-body aerodynamics and the structural modes. This

---

*Because of the sign convention of x (+ x toward the rear) and z (+ z up), a positive slope corresponds to a negative pitch angle.

procedure is similar to that used in handling qualities analysis to determine lower order equivalent systems where the higher order control-system dynamics are represented as a time delay.[4] The plausibility of such a delay can be visualized by considering an aircraft that has a wing with torsional flexibility. The initial result of a surface deflection will be a wing twisting. After the wing has twisted, aerodynamic forces will be generated, resulting in rigid-body pitch acceleration and longitudinal first-bending mode acceleration. This phenomenon was represented as a delay between the surface position as produced by the actuator and the surface position that is used to drive both the rigid and flexible responses. An additional delay was allowed for the acceleration response as shown in the following transfer functions:

$$\frac{\delta_d(s)}{\delta(s)} = e^{-\tau_\delta s}$$

$$\frac{q(s)}{\delta_d(s)} = \left[\frac{q_r(s)}{\delta_d(s)} + \frac{q_s(s)}{\delta_d(s)} \right]$$

$$\frac{A_n(s)}{\delta_d(s)} = \left[\frac{A_{ncg_r}(s)}{\delta_d(s)} + \frac{\Delta x}{g} \frac{\dot{q}_r(s)}{\delta_d(s)} + \frac{A_{n_s}(s)}{\delta_d(s)} \right] e^{-\tau_{a_n} s}$$

For the current SR-71 flight test program, there was no instrumentation for the control-surface positions. The control-surface responses were calculated using the simulation models for the actuators and the pilot control input, which was recorded. As a result, it was not possible to discriminate between delays caused by structural effects and delays caused by errors in the actuator models.

CALIBRATION TECHNIQUES USING TEST DATA

The unknown variables required to define the structural model are ω_s, ζ_s, FS_0, L, A_1, A_2, F_δ, τ_{a_n}, and τ_δ. Flight data were available for normal acceleration and pitch rate at two fuselage stations: one at FS 235, near the nose, and the other at FS 683, near the c.g. The best method to solve the unknown parameters is a parameter-estimation technique such as the pEst software,[5] which readily identify the unknown structural characteristics and the generally unknown rigid-body aircraft characteristics. The time delay can be estimated by shifting the input time history various amounts[6] or solved directly by using the nonlinear estimation capability of the pEst program.[5] For the SR-71 aircraft, the structural mode identification can also be accomplished with a simplified analysis because the structural mode frequency is sufficiently removed from the short-period frequency and the stability augmentation system is not significantly coupled with the structural mode because of the sensor location. In general, these conditions will not exist. The motivating factor for including the structural modes in the handling qualities analysis is that the structural frequency is near enough to the short-period frequency to cause a problem for pilot control. This also makes a simplified analysis difficult and generally can only be analyzed by using parameter-estimation techniques. The following section will develop the method used for the simplified analysis to provide some insight into the results.

Simplified Analysis Technique

The four mode shape parameters—FS_0, L, A_1, and A_2—can be determined from the ratios of the magnitudes of the two pitch-rate and two normal-acceleration responses. These ratios are A_n/q at the forward and aft locations, $A_{n_{fwd}}/A_{n_{aft}}$ and q_{fwd}/q_{aft}. When these ratios are obtained from the free-oscillation part of the response following a sharp excitation input, the response is primarily caused by the structure. From the previous expressions

for A_{n_s} and q_s, the ratios can be evaluated at the structural frequency ω_s. The phase information can be used to determine the location of the motion along the x-axis. When the positive A_{n_s} peak leads the positive q_s peak by 90°, the ratio $\left|\dfrac{A_{n_s}}{q_s}\right|$ is considered positive. The ratios $\left|\dfrac{A_{n_{s_{fwd}}}}{A_{n_{s_{aft}}}}\right|$ and $\left|\dfrac{q_{s_{fwd}}}{q_{s_{aft}}}\right|$ are considered positive when both responses are on the same side of the node. Figure 4 provides an example of the free-oscillation portion of a time history. In this example, the amplitude ratios can be read directly from the time history. However, in many cases, it was more difficult to directly measure the amplitudes because of the noise on the measurements. As a result, a curve fit of each parameter was made and the amplitudes were determined from the fitted curves.
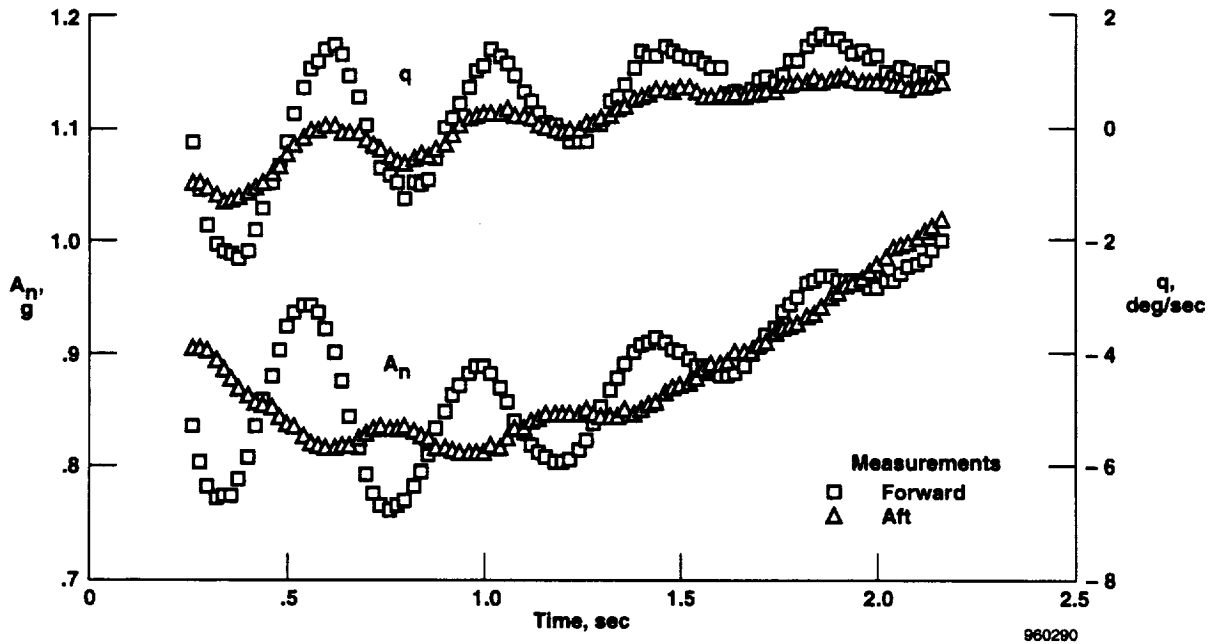
Figure 4. Free-oscillation portion of response to sharp pitch control input, M 0.8.

For the example time history, the measured value of the structural mode frequency was 14.6 rad/sec. The amplitude ratios from the measurements at the forward location (FS 234.5) and the aft location (FS 683) resulted in the following equations:

- Ratio of acceleration to pitch rate at the two fuselage stations

$$\left|\frac{A_{n_s}}{q_s}\right|_{fwd} = \frac{L}{12gA_2} \frac{\cos\left(1.5\pi\dfrac{(234.5 - FS_0)}{12L}\right) - A_1}{\sin\left(1.5\pi\dfrac{(234.5 - FS_0)}{12L}\right)} \quad 14.6 = 0.058 \ g/\deg/\sec$$

$$\left|\frac{A_{n_s}}{q_s}\right|_{aft} = \frac{L}{12gA_2} \frac{\cos\left(1.5\pi\dfrac{(683 - FS_0)}{12L}\right) - A_1}{\sin\left(1.5\pi\dfrac{(683 - FS_0)}{12L}\right)} \quad 14.6 = -0.034 \ g/\deg/\sec$$

- Ratio of accelerations at forward and aft fuselage stations

$$\left|\frac{A_{n_{S_{fwd}}}}{A_{n_{S_{aft}}}}\right| = \frac{\cos\left(1.5\pi\frac{(234.5 - FS_0)}{12L}\right) - A_1}{\cos\left(1.5\pi\frac{(683 - FS_0)}{12L}\right) - A_1} = -5.72$$

- Ratio of pitch rates at the forward and aft fuselage stations

$$\left|\frac{q_{S_{fwd}}}{q_{S_{aft}}}\right| = \frac{\sin\left(1.5\pi\frac{(234.5 - FS_0)}{12L}\right)}{\sin\left(1.5\pi\frac{(683 - FS_0)}{12L}\right)} = 3.40$$

These equations were then solved for the four unknowns L, FS_0, A_1, and A_2. The solution required an iterative procedure, and a spreadsheet with an equation solver was used for this process. Good starting values for the solution are L = fuselage length and $FS_0 = L/2$. Figure 5 shows the solution. It can be seen that the assumption of the sinusoidal form for the deflection distribution provides a rather nonlinear solution obtained from a minimum number of measurements. The next step was to determine the structural gain F_δ and the time delays. This was accomplished by putting the mode shape data into the simulation and then adjusting the gain and delays to obtain the best fit to the flight data. The delays were adjusted only to the nearest simulation frame (0.020 sec). The delay in the elevator control input, determined from the pitch-rate response, was found to be 3 frames or 0.060 sec. A 4-frame delay (0.080 sec) had to be added to the normal-acceleration responses. This is likely caused by delays in the accelerometer instrumentation itself rather than any structural phenomena.
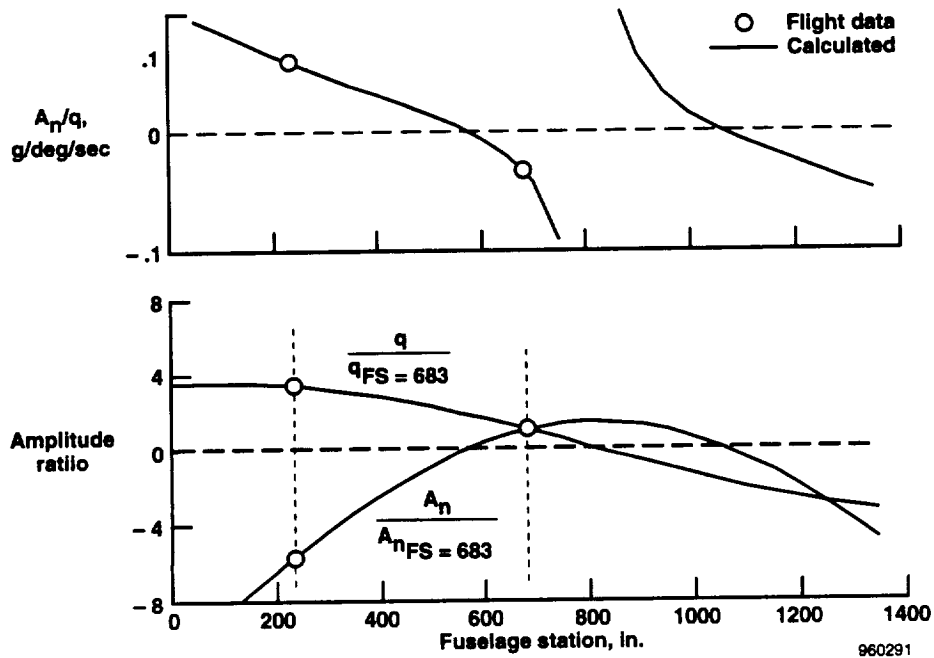

Figure 5. Pitch-rate and normal-acceleration amplitude ratios and calculated fit.

9

Parameter-Estimation Techniques

Two parameter-estimation techniques were used: the pEst software[5] and the spreadsheet identification method, which uses the equation solving capability of a spreadsheet on a personal computer. These techniques use the longitudinal short-period rigid-body equations of motion and structural equations of motion. The input to the system of equations was the elevator deflection. Because the elevator deflection was not measured in flight, a calculated value was obtained by using the measured stick position and the simulation to obtain the elevator position. The elevator position was the average of the inboard and outboard elevator positions. The simulation actuator models were second order, with the inboard elevator driven by the stick command and the outboard elevator driven by the inboard elevator position. The elevator input to the aerodynamic and structural models was delayed by τ_δ so that the input at time t was $\delta(t - \tau_\delta)$. The following equations were used to model the dynamic responses:

$$\dot{q}_r(t) = M_q\, q_r(t) + M_\alpha\, \alpha_r(t) + M_\delta\, \delta(t - \tau_\delta) + M_0$$

$$\dot{\alpha}_r(t) = q_r(t) - L_\alpha\, \alpha_r(t) - L_\delta\, \delta(t - \tau_\delta) + L_0$$

$$\ddot{\eta}(t) = -2\,\zeta\,\omega\,\dot{\eta}(t) - \omega^2\,\eta(t) + \omega^2\, F_\delta\, \delta(t - \tau_\delta) + F_0$$

The output equations were as follows:

$$A_n(t) = \frac{V}{g}\left(q_r\!\left(t - \tau_{a_n}\right) - \dot{\alpha}_r\!\left(t - \tau_{a_n}\right)\right) + \frac{\Delta x}{g}\dot{q}_r\!\left(t - \tau_{a_n}\right) + \frac{1}{12g}\left[-\cos\!\left(1.5\pi\frac{(FS - FS_0)}{12L}\right) + A_1\right]\ddot{\eta}\!\left(t - \tau_{a_n}\right) + A_{n_0}$$

$$q(t) = q_r(t) + \left[\frac{-A_2}{L}\sin\!\left(1.5\pi\frac{(FS - FS_0)}{12L}\right)\right]\dot{\eta}(t) + q_0$$

where FS and Δx were evaluated for the forward and aft instrument locations.

The cost function was the square of the difference between the calculated outputs and the flight-measured values of the four measurements. The unknown variables used to minimize the cost function were the structural coefficients, short-period rigid-body coefficients, and various bias terms: ω, ζ, F_δ, L, FS_0, A_1, A_2, τ_δ, τ_{a_n}, M_q, M_α, M_δ, L_α, L_δ, V, L_0, M_0, F_0, $A_{n_{0_{fwd}}}$, $A_{n_{0_{aft}}}$, $q_{0_{fwd}}$, $q_{0_{aft}}$.

For the spreadsheet solution, the time delay was determined by evaluating the cost function for various time delays, which were incremented as multiple sample intervals.[6] This was done for only one flight condition, and the results were used for the other conditions. For the pEst technique, the time delays were implemented as interpolated values of tables (i.e., δ as a function of time) and the time delay was estimated directly for each time history. With both techniques, the parameters of the nonlinear mode shape could be solved for directly. Other parameter-estimation techniques that require linear equations could be used by estimating K_1 and K_2 for the forward and aft location. The mode shape parameters L, FS_0, A_1, A_2 could then be calculated from K_1 and K_2.

Figure 6 provides a comparison of the mode shapes obtained from the simplified analysis results and the parameter-estimation technique results. All of the results show good agreement in the area of interest from the nose to the c.g. Some disagreement is seen at the aft end of the aircraft; however, if this area were of importance, additional instrumentation could be added in this region. Figure 7 shows a typical example of the fit of the flight data using the spreadsheet parameter-estimation technique for a flight condition at M 3.0. A reasonably good fit was generally obtained for all the flight conditions.

10
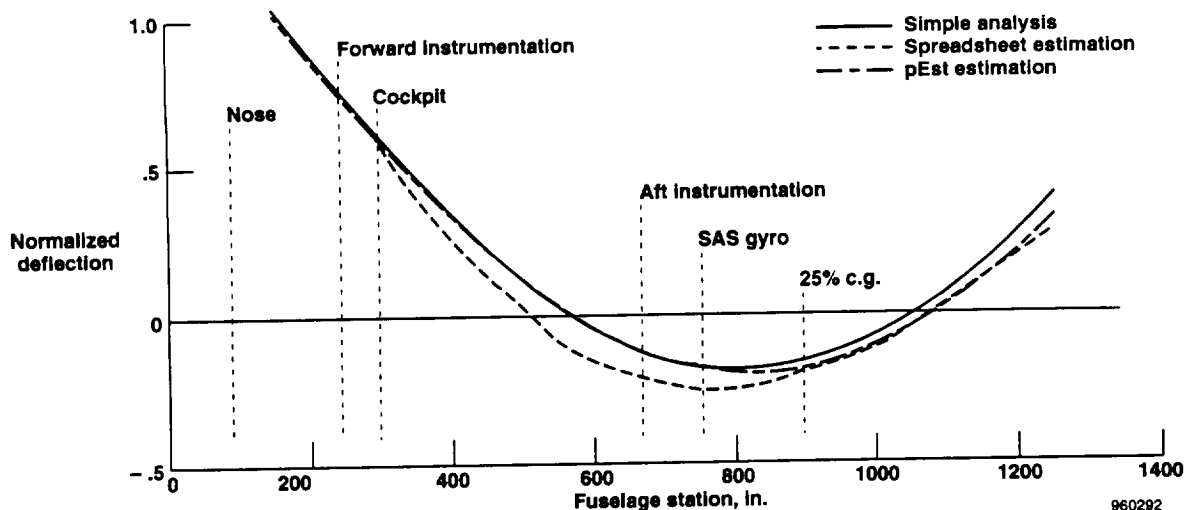
Figure 6. Comparison of mode shapes resulting from three analysis techniques, M 0.8.

SUMMARY OF PARAMETER-ESTIMATION RESULTS

The data used to analyze the structural characteristic data were collected on five flights of the SR-71 airplane. The maneuvers consisted of sharp raps of the longitudinal control stick, which primarily excited the structural mode. In one case, a frequency sweep maneuver was performed. A summary of the flight conditions and maneuvers is contained in table 1. The maneuvers at M 3.0 were performed with the stability augmentation on; the other maneuvers were performed with the stability augmentation off. The following discussion will present the results obtained from the five flights for the simplified analysis, spreadsheet parameter identification analysis, and pEst parameter identification analysis.

Table 1. Flight conditions for the test maneuvers.

| Flight	Maneuver	Mach number	Altitude, ft	Dynamic pressure, lb/ft^2	Aircraft weight, lb
15	Stick rap 1	0.785	20,200	440	72,900
15	Stick rap 2	0.800	19,800	440	72,400
18	Stick rap 1	0.825	18,000	490	120,000
18	Stick rap 2	0.825	18,400	490	119,900
18	Stick rap 3	0.825	18,700	490	119,800
19	Stick rap 1	0.850	22,800	400	115,900
19	Stick rap 2	0.850	23,200	445	115,800
20	Stick rap 1	0.800	20,600	426	11,750
20	Stick rap 2	0.820	21,000	440	117,100
20	Stick rap 3	0.830	21,200	447	116,700
21	Stick rap 1	3.000	75,300	460	80,300
21	Frequency sweep	3.000	75,300	460	80,000
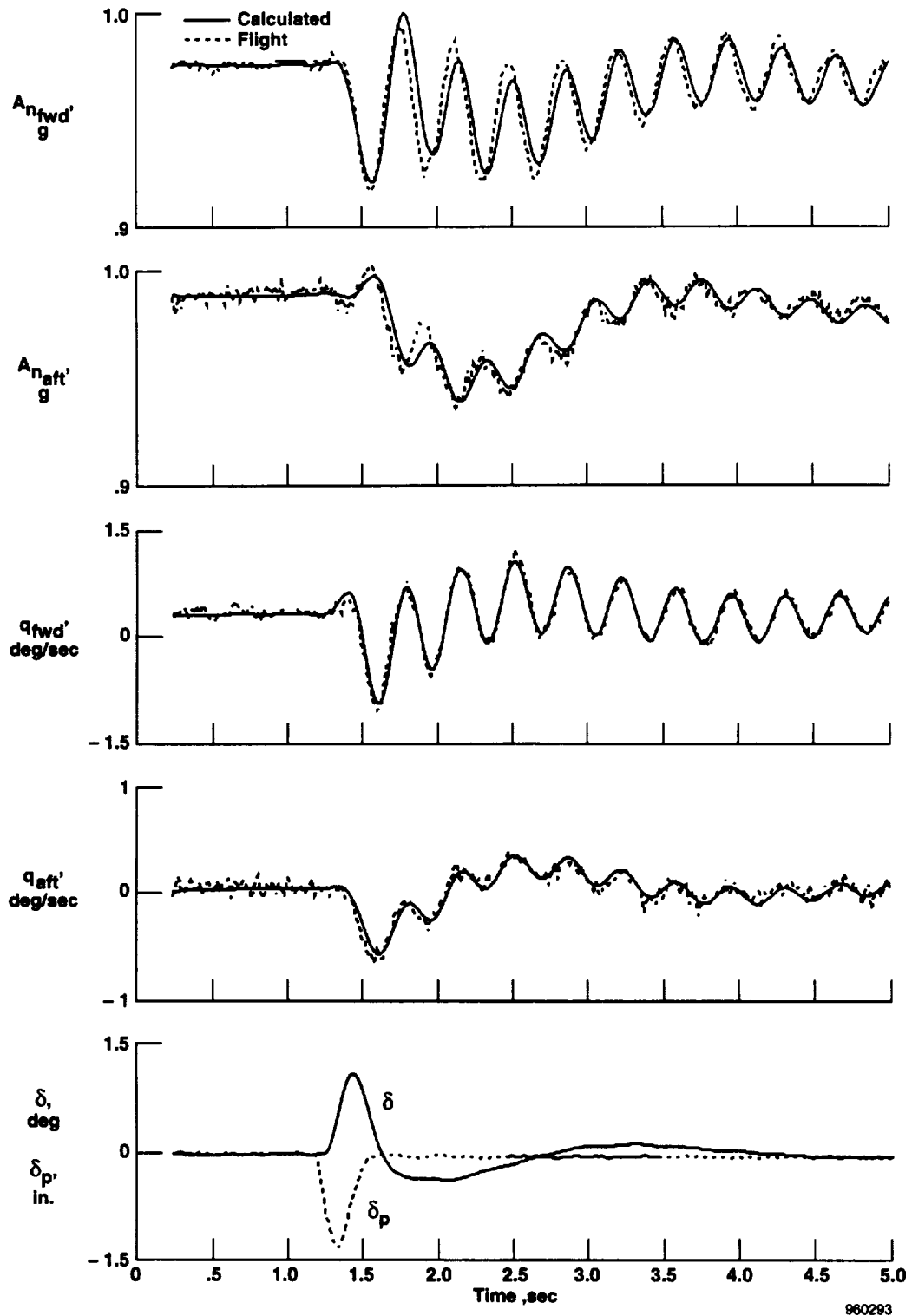
Figure 7. Time history of match between flight data and calculated time history using spreadsheet identification technique, M 3.0.

Mode Shape

Figure 8 shows the results of all the points in terms of the mode shape parameters L, FS_0, A_1, and A_2. The simplified analysis and the two parameter identification technique results showed good agreement, although the parameter identification results were usually more consistent. Good agreement was found between the spreadsheet
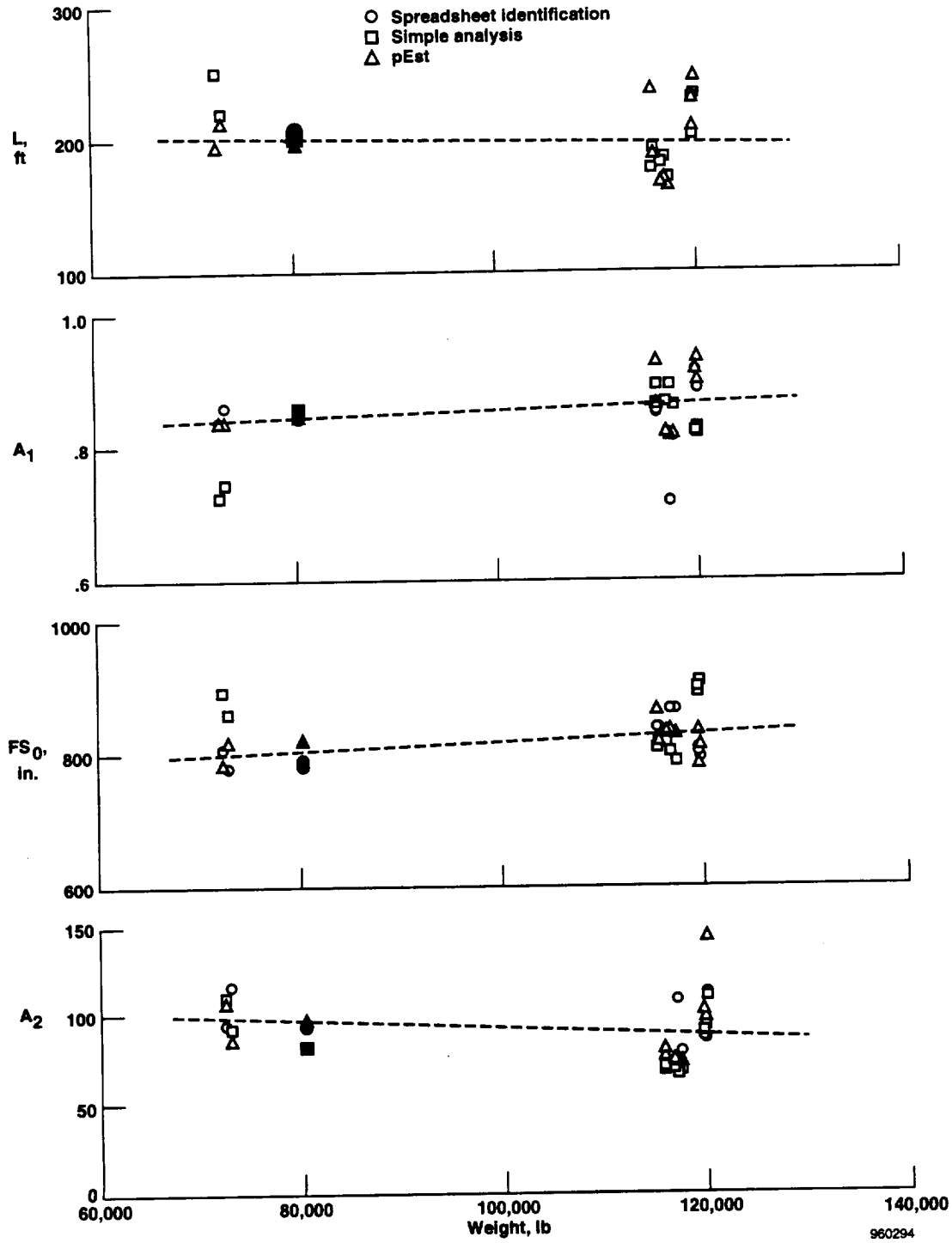

Figure 8. Mode shape parameters L, A_1, FS_0, and A_2 as function of aircraft gross weight, (open symbol, M 0.8; solid symbol, M 3.0).

13

parameter-estimation technique and the pEst technique. The faired line shown in figure 8 is a least square fit of the two sets of parameter identification data. The parameters FS_0 and A_1 were the most significant in determining the mode shape. Figure 9 shows the effect of the parameter variations with weight on the mode shape for two weight conditions. A fairly large shift in the forward node toward the aft is seen as the gross weight is increased.
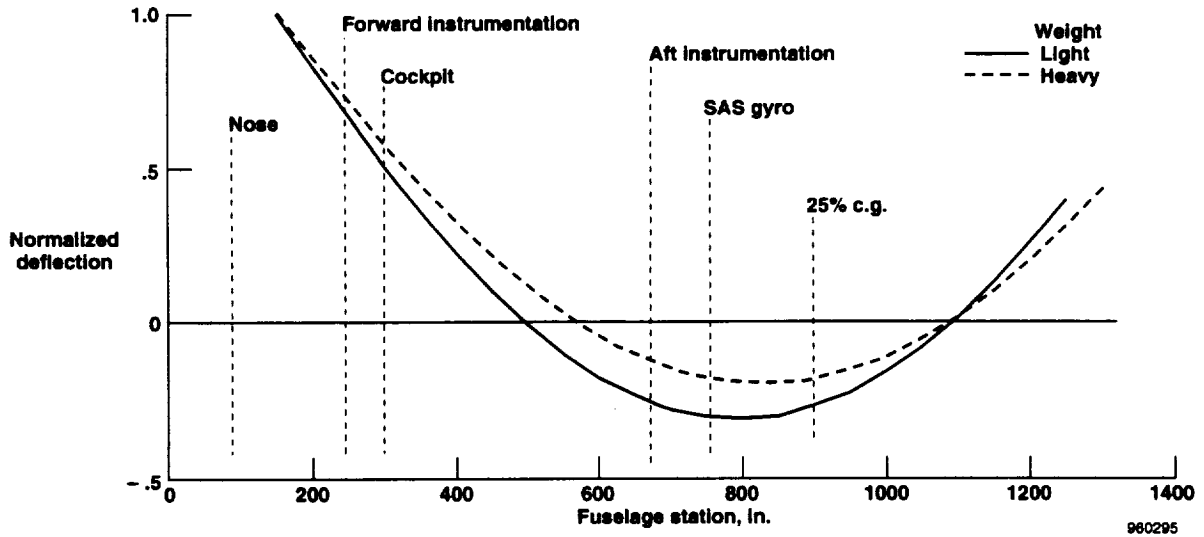
Figure 9. Comparison of mode shapes for heavy-weight and lightweight aircraft using faired data from figure 8.

Control Effectiveness

Figure 10 shows the control effectiveness parameter. The control effectiveness was modeled as $F_\delta = \frac{\bar{q} S}{W} C_{F_\delta}$. It would be expected that the control effectiveness for the structural mode would be similar to the control effectiveness for the rigid-body motion. A curve proportional to pitching moment caused by elevator is shown in figure 10. The flight data are in general agreement with this trend although data as a function of Mach number are very
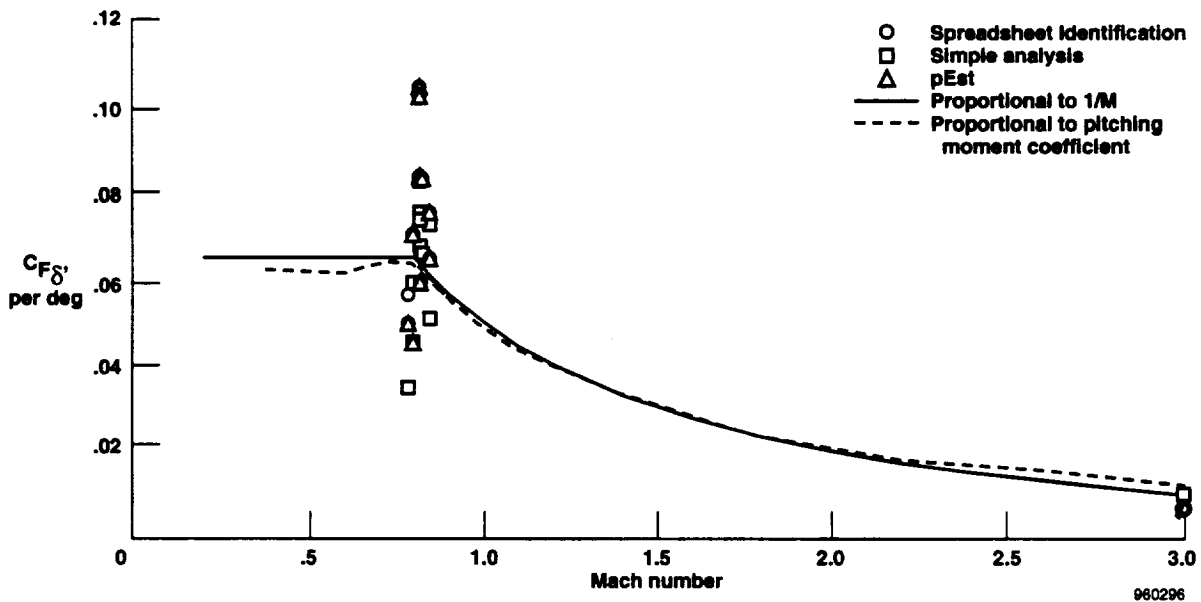
Figure 10. Structural control effectiveness parameter.

14

limited. A simple approximation to this function of Mach number is a function inversely proportional to Mach number with an upper limit, as shown in figure 10.

Frequency and Damping

Figure 11 shows the structural frequency and damping. The frequency was a function of vehicle gross weight but was not significantly affected by flight condition. The damping ratio was independent of airplane gross weight but was noticeably reduced at the M 3.0 flight condition. Figure 12 shows the decrease in damping with Mach number. A function similar to the one used for the control effectiveness is also shown as an interpolation over the
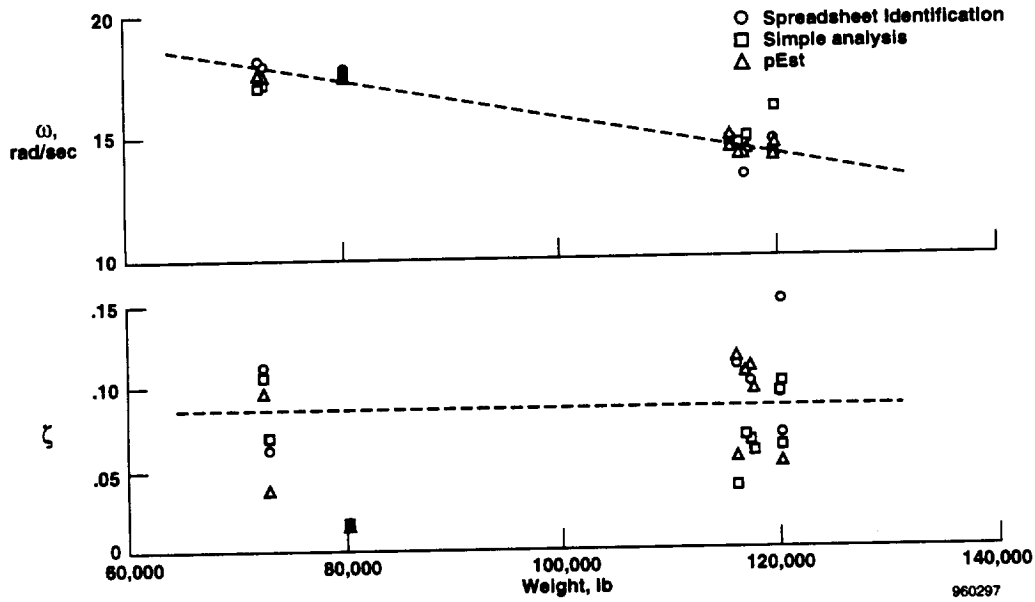
Figure 11. Structural frequency and damping characteristics as function of airplane weight (open symbol, M 0.8; solid symbol, M 3.0).
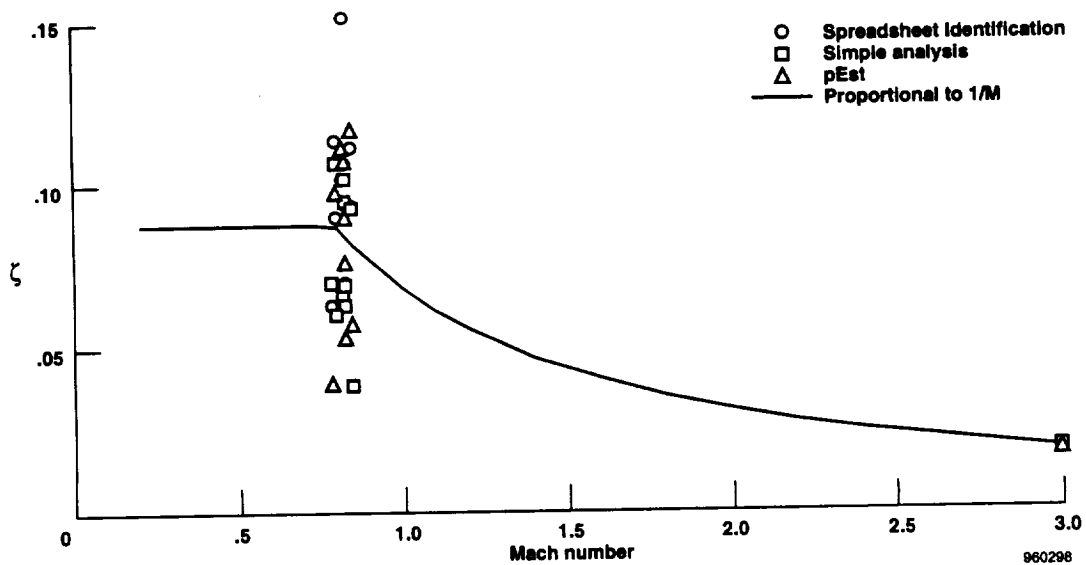
Figure 12. Structural damping characteristics as function of Mach number.

15

Mach number range; however, there are only marginal data to support this trend. No effect on damping was seen because of dynamic pressure over the limited range tested.

Time Delay

The time delay was estimated with the spreadsheet parameter-estimation technique at one flight condition. Several fits were obtained using a range of time delays for both the elevator and the normal acceleration. Table 2 lists the cost function results from the matches. An interpolation of these data produced an estimate for the elevator delay of τ_δ = 0.064 sec and τ_{a_n} = 0.077 sec. It can be seen that the simplified analysis estimate of a 3-frame delay (0.060 sec) for the elevator and a 4-frame delay (0.080 sec) for the normal acceleration agrees well with the spreadsheet parameter-estimation results at the same flight condition. An easier estimation of the time delay was obtained from the pEst program, which had the capability to directly estimate the time delays for each maneuver. Figure 13 shows the three sets of results. Considerably more scatter is seen when all of the pEst points are included. The pEst results indicated an average elevator time delay of τ_δ = 0.036 sec and an average normal-acceleration time delay of τ_{a_n} = 0.100 sec.

Table 2. Cost function from the spreadsheet parameter estimation as a function of pitch-rate and normal-acceleration time delays.

		τ_{a_n}, sec		
		0.06	0.08	0.10
	0.04	18.5771	16.2385	20.1536
τ_δ, sec	0.06	12.2156	10.696	13.9351
	0.08	14.7924	13.6397	16.7074
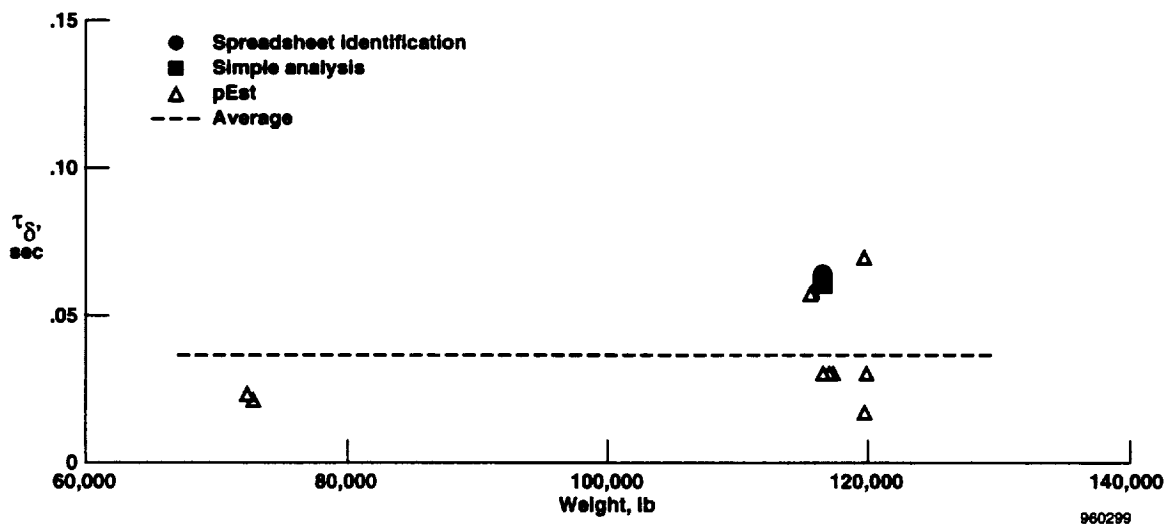
(a) Elevator.

Figure 13. Elevator and normal-acceleration time delays.

16
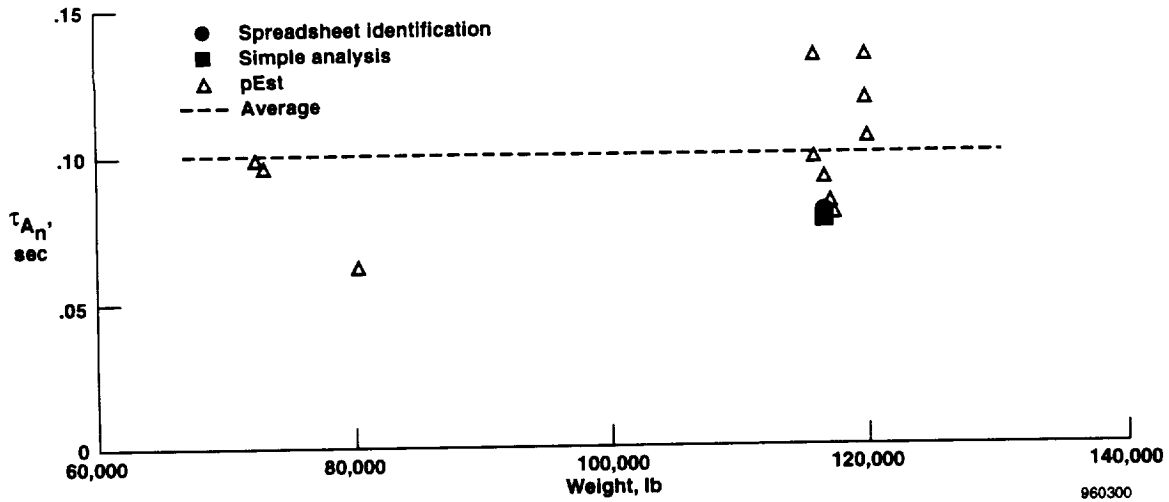
(b) Normal acceleration.

Figure 13. Concluded.

SIMULATION RESULTS

Simulation Model

A simulation model of the longitudinal first-bending mode was created from the parameter estimation results. The structural mode equations were added to the rigid-body states. A low-pass filter was used to approximate the steady-state trim elevator deflection. The incremental elevator deflection, which is the input to the structural mode model, is the difference between the current and the filtered elevator positions. The transfer functions for the structural motion and the combination with the rigid-body motion are shown in the following equations as a function of the fuselage station:

$$\Delta\delta(s) = \left(1 - \frac{0.1}{s + 0.1}\right)\delta(s)$$

$$\frac{A_{n_s}(s)}{\Delta\delta(s)} = \frac{1}{12g}\left[-\cos\left(1.5\pi\frac{FS - FS_0}{12L}\right) + A_1\right]\left[\frac{s^2\,\omega^2}{s^2 + 2\zeta\omega s + \omega^2}\right]F_\delta$$

$$\frac{q_s(s)}{\Delta\delta(s)} = \left[\frac{-A_2}{L}\sin\left(1.5\pi\frac{FS - FS_0}{12L}\right)\right]\left[\frac{s\,\omega^2}{s^2 + 2\omega\zeta s + \omega^2}\right]F_\delta$$

$$\frac{A_n(s)}{\delta(s)} = \left[\frac{A_{n_{cg_r}}(s)}{\delta(s)} + \frac{\Delta x}{g}\frac{\dot{q}_r(s)}{\delta(s)} + \frac{A_{n_s}(s)}{\Delta\delta(s)}\right]e^{-\tau_{a_n}s}\,e^{-\tau_\delta s}$$

$$\frac{q(s)}{\delta(s)} = \left[\frac{q_r(s)}{\delta(s)} + \frac{q_s(s)}{\Delta\delta(s)}\right]e^{-\tau_\delta s}$$

17

The control effectiveness was modeled as a function of Mach number and dynamic pressure as follows:

$$C_{F_\delta} = 0.06 / M - 0.01$$

$$C_{F_\delta} < 0.065$$

$$F_d = \frac{\bar{q}S}{W} C_{F_\delta}$$

The structural mode shape parameters were modeled as a function of airplane gross weight as follows:

$$L = 208 - 0.000105\,W$$

$$FS_0 = 752 + 0.00063\,W$$

$$A_1 = 0.803 + 0.00000049\,W$$

$$A_2 = 113 - 0.000214\,W$$

As shown below, the structural frequency was modeled as a function of airplane gross weight, and the structural damping ratio was varied as a function of Mach number:

$$\omega_s = 23.6 - 0.000079\,W$$

$$\zeta_s = 0.075 / M - 0.007$$

$$\zeta_s < 0.087$$

The time delays were modeled as pure time delays with the following values:

$$\tau_\delta = 0.036\ \text{sec}$$

$$\tau_{a_n} = 0.100\ \text{sec}$$

Comparison of Flight/Simulation Frequency Response

The frequency response characteristics are of particular interest for handling qualities analysis. A frequency sweep maneuver was performed in flight at M 3.0, and this was used to compare the results from the simulation model that was developed with the flight data. The stick input from the flight maneuver was used to produce a simulation time history of the frequency sweep maneuver. Fast-Fourier transforms were used on both the flight and simulated data to find the pitch rate and normal acceleration to pilot input transfer functions. Figure 14 shows the results for the forward instrumentation location, and figure 15 shows the results for the aft instrumentation location. The simulation model shows reasonably good agreement with the flight data at the M 3.0 flight condition. The simulation model also allows the extrapolation to other fuselage locations. Figure 16 shows the frequency response characteristics for the pilot location, which are of interest for handling qualities analysis. Figure 16 also shows the original rigid-body responses from the simulation. Significant improvements in the model fidelity are shown in the higher frequency region, especially for the pitch-rate response. The results indicate that the desired objective, to provide a model suitable for handling qualities analysis which includes the structural dynamic effects, has been achieved.

18
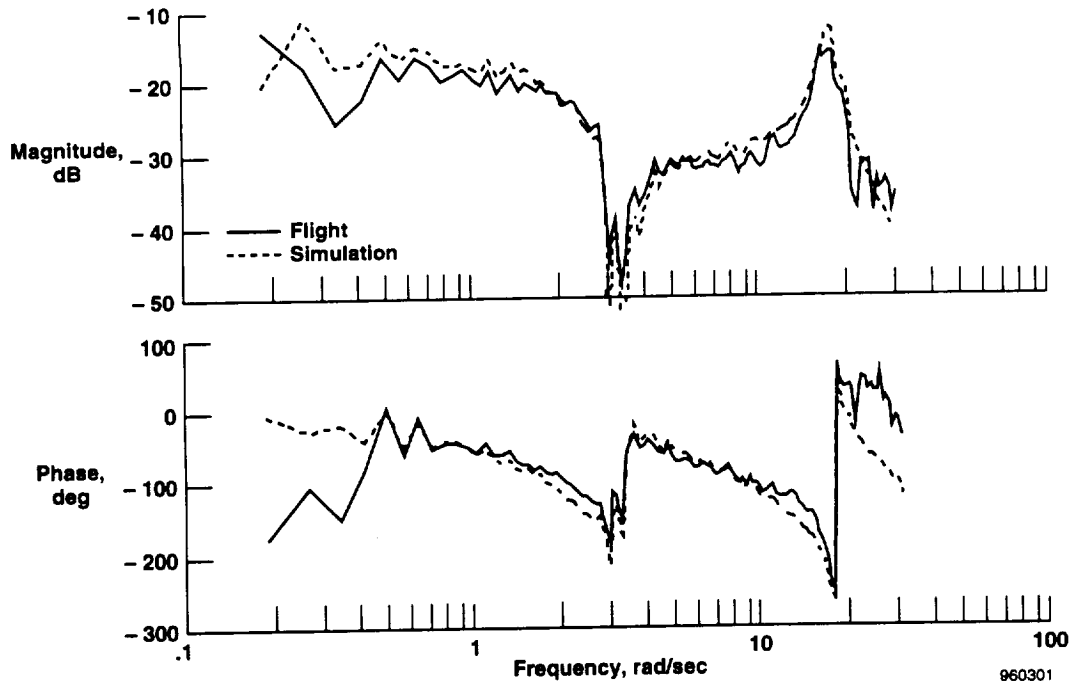
(a) Normal acceleration for pilot stick input.
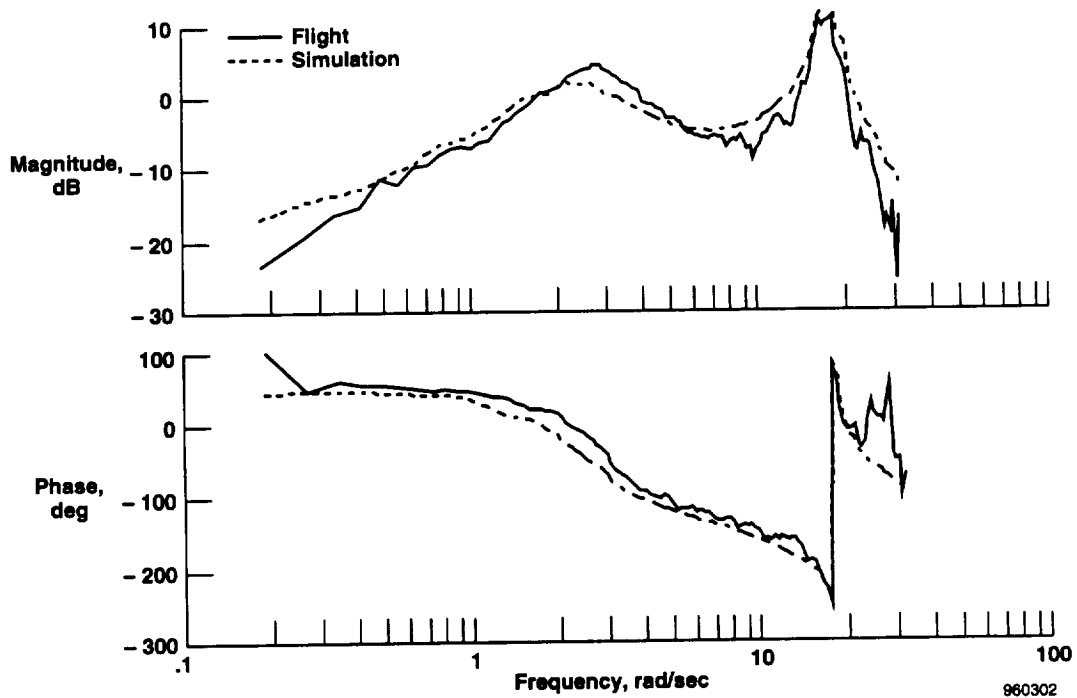
(b) Pitch rate for pilot stick input.

Figure 14. Comparison of normal-acceleration and pitch-rate transfer functions from flight and simulation for forward-sensor location at M 3.0.

19
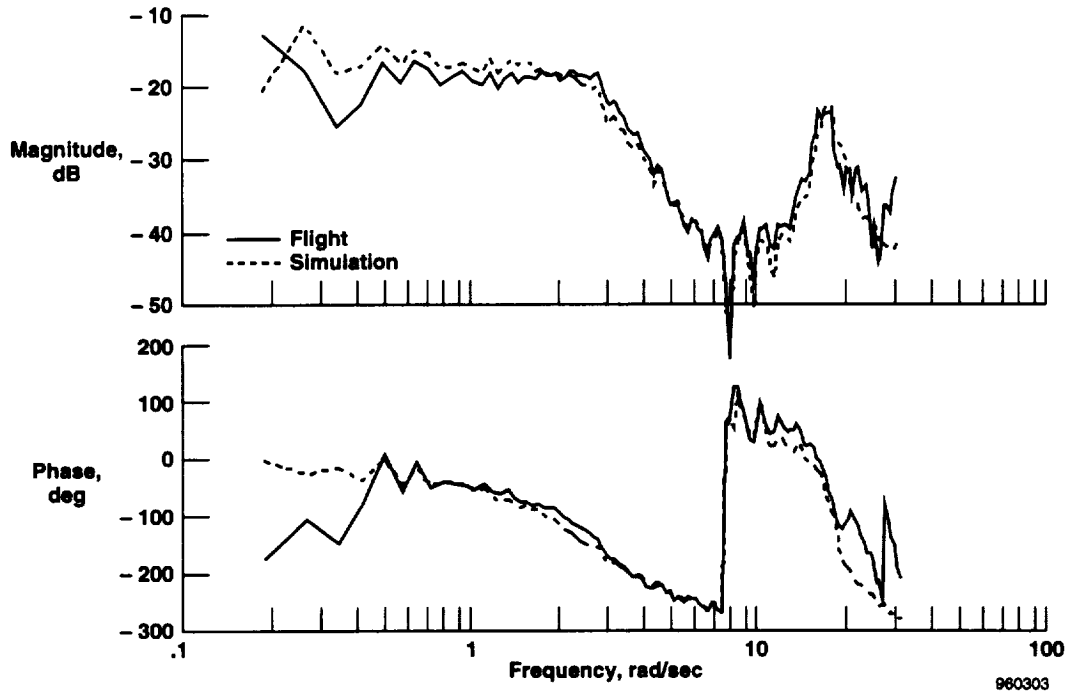
(a) Normal acceleration for pilot stick input.
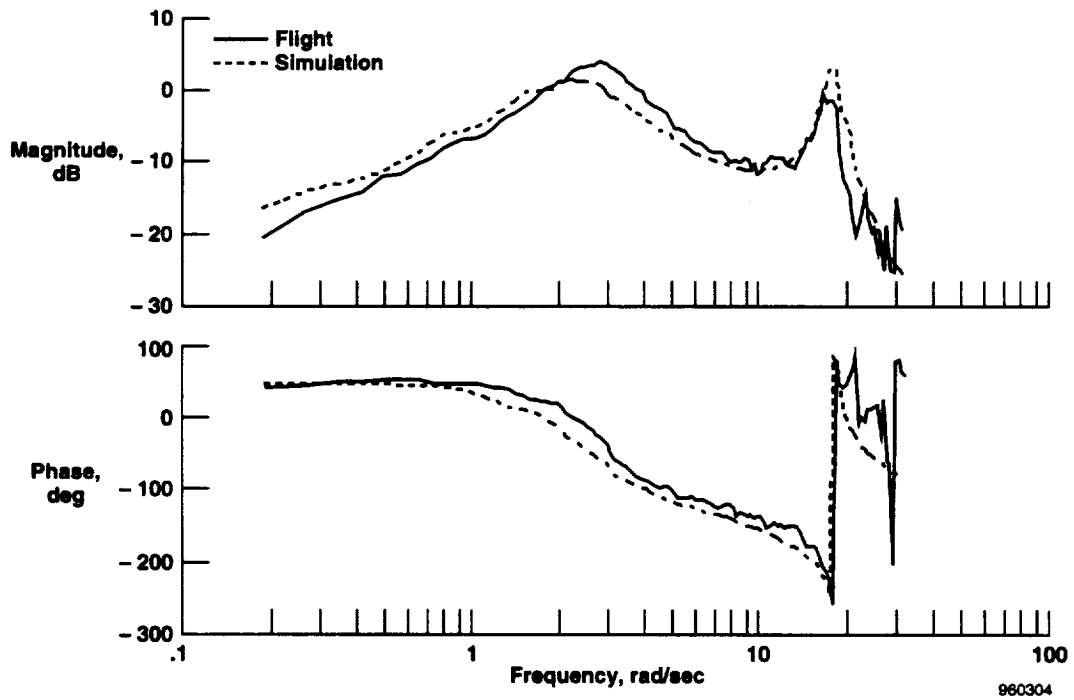
(b) Pitch rate for pilot stick input.

Figure 15. Comparison of normal-acceleration and pitch-rate transfer functions from flight and simulation for aft-sensor location at M 3.0.

20
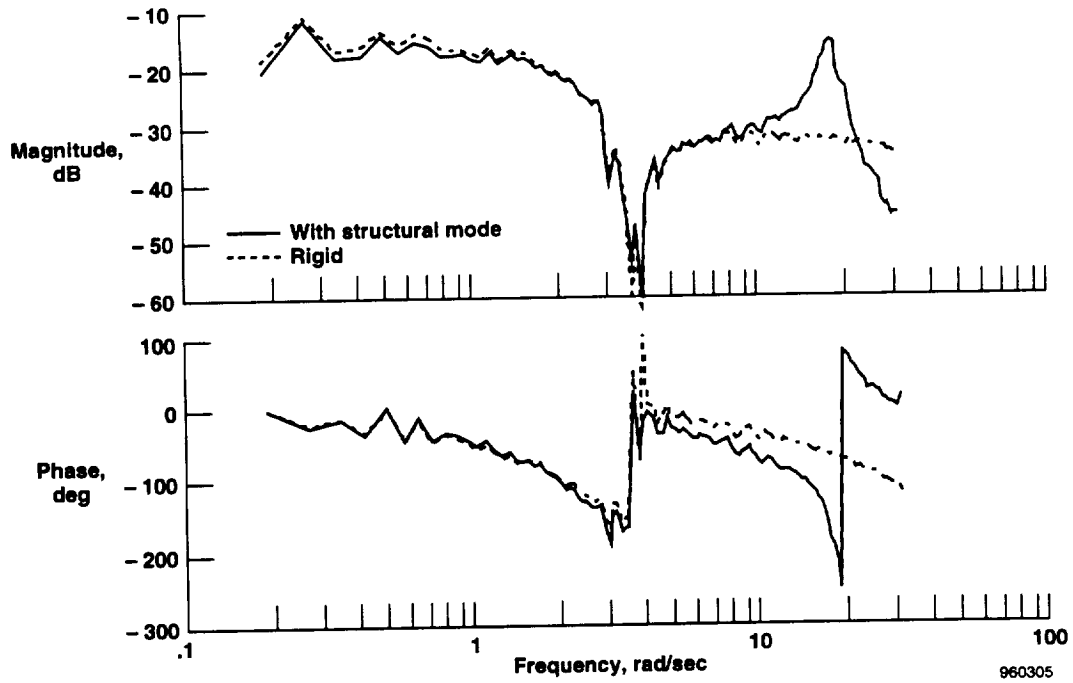
(a) Normal acceleration for pilot stick input.
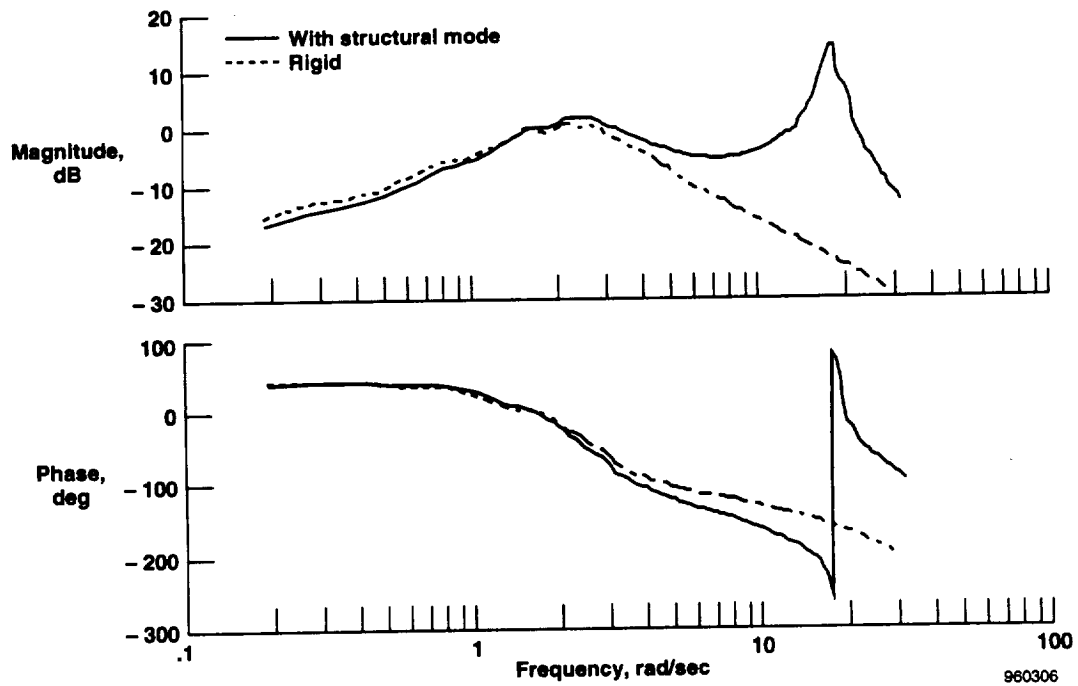
(b) Pitch rate for pilot stick input.

Figure 16. Simulation results for normal-acceleration and pitch-rate transfer functions for pilot location at M 3.0.

CONCLUDING REMARKS

The ability to use flight data to determine an aircraft model with structural dynamic effects suitable for piloted simulation and the analysis of handling qualities and flight control system has been developed. This technique was demonstrated using SR-71 flight test data. For the SR-71 aircraft, the most significant structural response is the longitudinal first-bending mode. This mode was modeled as a second-order system. The effect of other higher order modes was modeled as a time delay to both the rigid-body and structural motion. The distribution of the modal response at various fuselage locations was developed using a uniform beam solution, which can be calibrated using flight data. This approach was compared with the mode shape obtained from GVT, and the general form of the uniform beam solution was found to be a good representation of the mode shape in the areas of interest. A simplified analysis calibration technique was developed and is applicable when structural dynamic motion is not significantly altered by the control system and is separated significantly from the rigid-body motion. For the more difficult case, where the control-system or short-period interactions prevent a simple analysis, a parameter-estimation technique was demonstrated. This analysis can be accomplished by using either standard parameter-estimation programs or a personal computer spreadsheet analysis with equation solving capability. To calibrate the uniform beam solution, pitch-rate and normal-acceleration instrumentation is required for at least two locations. This technique provided structural mode shape information that is comparable to a GVT with a minimum of instrumentation, flight time, and analysis. With the resulting structural model incorporated into the simulation, a good representation of the flight characteristics was provided for handling qualities and control-system analyses.

REFERENCES

[1]Waszak, Martin R., John B. Davidson, and David K. Schmidt, *A Simulation Study of the Flight Dynamics of Elastic Aircraft*, NASA CR 4102, 1987.

[2]Freeberg, C.R. and E.N. Kemler, *Elements of Mechanical Vibration*, New York: Wiley & Sons, 1960.

[3]Smith, John W. and Donald T. Berry, *Analysis of Longitudinal Pilot-Induced Oscillation Tendencies of YF-12 Aircraft*, NASA TN D-7900, 1975.

[4]Hodgkinson, J. and W.J. LaManna, *Equivalent System Approaches to Handling Qualities Analysis and Design Problems of Augmented Aircraft*, AIAA 77-1122, Aug. 1977.

[5]Murray, James E. and Richard E. Maine, *pEst version 2.1 User's Manual*, NASA TM-88280, 1987.

[6]Shafer, M.F., *Low-Order Equivalent Models of Highly Augmented Aircraft Determined from Flight Data*, J. Guidance, Control, and Dynamics, AIAA 80-1627R, Sept.–Oct. 1982.

REPORT DOCUMENTATION PAGE

Form Approved
OMB No. 0704-0188

1. AGENCY USE ONLY (Leave blank)	2. REPORT DATE	3. REPORT TYPE AND DATES COVERED
	June 1996	Technical Memorandum

4. TITLE AND SUBTITLE

Structural Dynamic Model Obtained From Flight for Use With Piloted Simulation and Handling Qualities Analysis

5. FUNDING NUMBERS

WU 537-09-22

6. AUTHOR(S)

Bruce G. Powers

7. PERFORMING ORGANIZATION NAME(S) AND ADDRESS(ES)

NASA Dryden Flight Research Center
P.O. Box 273
Edwards, California 93523-0273

8. PERFORMING ORGANIZATION REPORT NUMBER

H-2075

9. SPONSORING/MONOTORING AGENCY NAME(S) AND ADDRESS(ES)

National Aeronautics and Space Administration
Washington, DC 20546-0001

10. SPONSORING/MONITORING AGENCY REPORT NUMBER

NASA TM-4747

11. SUPPLEMENTARY NOTES

Bruce G. Powers, Analytical Services and Material, Inc., Edwards, California

12a. DISTRIBUTION/AVAILABILITY STATEMENT

Unclassified—Unlimited
Subject Category 08

12b. DISTRIBUTION CODE

13. ABSTRACT (Maximum 200 words)

The ability to use flight data to determine an aircraft model with structural dynamic effects suitable for piloted simulation and handling qualities analysis has been developed. This technique was demonstrated using SR-71 flight test data. For the SR-71 aircraft, the most significant structural response is the longitudinal first-bending mode. This mode was modeled as a second-order system, and the other higher order modes were modeled as a time delay. The distribution of the modal response at various fuselage locations was developed using a uniform beam solution, which can be calibrated using flight data. This approach was compared to the mode shape obtained from the ground vibration test, and the general form of the uniform beam solution was found to be a good representation of the mode shape in the areas of interest. To calibrate the solution, pitch-rate and normal-acceleration instrumentation is required for at least two locations. With the resulting structural model incorporated into the simulation, a good representation of the flight characteristics was provided for handling qualities analysis and piloted simulation.

14. SUBJECT TERMS

Handling qualities; Parameter estimation; Simulation; Structural dynamics

15. NUMBER OF PAGES

25

16. PRICE CODE

A03

17. SECURITY CLASSIFICATION OF REPORT	18. SECURITY CLASSIFICATION OF THIS PAGE	19. SECURITY CLASSIFICATION OF ABSTRACT	20. LIMITATION OF ABSTRACT
Unclassified	Unclassified	Unclassified	Unlimited

National Aeronautics and
Space Administration
Code JTT
Washington, D.C. 20546-0001
USA

Official Business
Penalty for Private Use, $300

POSTMASTER: If Undeliverable (Section 158
Postal manual) Do Not Return